X International Conference on Computational Methods in Marine Engineering
MARINE 2023
J. Garcia-Espinosa, L. González, J.E. Gutiérrez & B. Serván-Camas (Editors)

Model basin testing of a floating solar system compared to analysis for establishment of design verification culture

MARINE 2023

1. Are J. Berstad* and Petter Grøn†

* Aquastructures
Kjøpmannsgata 21, N-7013 Trondheim, Norway
e-mail: are@aquastructures.no, web page: http://www.aquasim.no

† Ocean Sun
Snarøyveien 20, N-1360 Fornebu, Norway
Email: pg@oceansun.no - Web page: http://www.oceansun.no

.

Keywords: Floating solar; Model basin testing; Finite element analysis; Hydrodynamics; Hydroelasticity; Wave theory.

NOMENCLATURE

A	Area[m^2]
u	Fluid velocity [m/s]
λ	Wave length [m]
k	Wave number = $2\pi/\lambda$ [m^{-1}]
F	Force [N]
h	Height from bottom to water line [m]
ζ_a	Wave elevation [m]
ρ	Fluid density [kg m^{-3}]
a	Fluid acceleration [ms^{-2}]
ω	Wave frequency [s^{-1}]
C_d	Drag coefficient
C_s	Tangential friction / suction coefficient, linear
C_{at}	Tangential added mass coefficient
C_t	Tangential drag coefficient.

ABSTRACT

This paper presents analyses compared to model basin testing for a floating solar panel system as seen in Figure 1. The analyses are based on Finite Element Method (FEM) to represent the flexibility of the system (Aquastructures 2022). Loads based on hydrodynamic theory from waves and currents are applied in a time domain simulation to calculate coupled response from tarpaulin, floating collars and moorings. The analysis uses FE elements suitable for tarpaulins distributed along the water surface. (‘surface tarpaulin’). The paper presents a theory to hydroelastically calculate loads and responses for

surface tarpaulins. Basic loads such as drag and pressure from hydrostatic and hydrodynamic loads are included. The paper presents the surface suction effect occurring between the water surface and the tarpaulin giving forces in the horizontal plane of the surface. Theory for parallel surface suction effect is outlined and a practical way to include this in analysis is presented.

The paper presents a model basin test case of a realistic configuration. This is used for comparing response calculated by analysis to the findings in the model basin. Results show good correspondence. Sensitivity studies are carried out and guidance regarding how the results from this paper may be applied for actual design verifications of surface tarpaulin membranes carrying solar panels is discussed.

1. INTRODUCTION

A floating photovoltaic (FPV) solar panel system based on Ocean Sun's patented elastic membrane technology is shown in Figure 1. The FPV floater consists of c-Si PV modules attached on a surface tarpaulin, where the surface tarpaulin is confined by a flexible floating collar.

Figure 1 Floating surface tarpaulin with solar panels. (Ocean Sun 2018)

Hydroelastic analysis of the coupled system with tarpaulin, floating collars and moorings are carried out ahead of each installation of the FPV system to find system integrity (Aquastructures 2022). Model basin tank testing has been carried out to validate analysis. Scale model tests with a 1:16 Froude scaled model of an Ocean Sun OS-50 floating solar platform were carried out in the large towing tank at Sintef Ocean. Regular and irregular waves were tested, as well as free decay tests and towing. All experimental and numerical results herein are presented in model scale. Figure 2 shows a part of the test setup in the model basin (Sintef 2021).

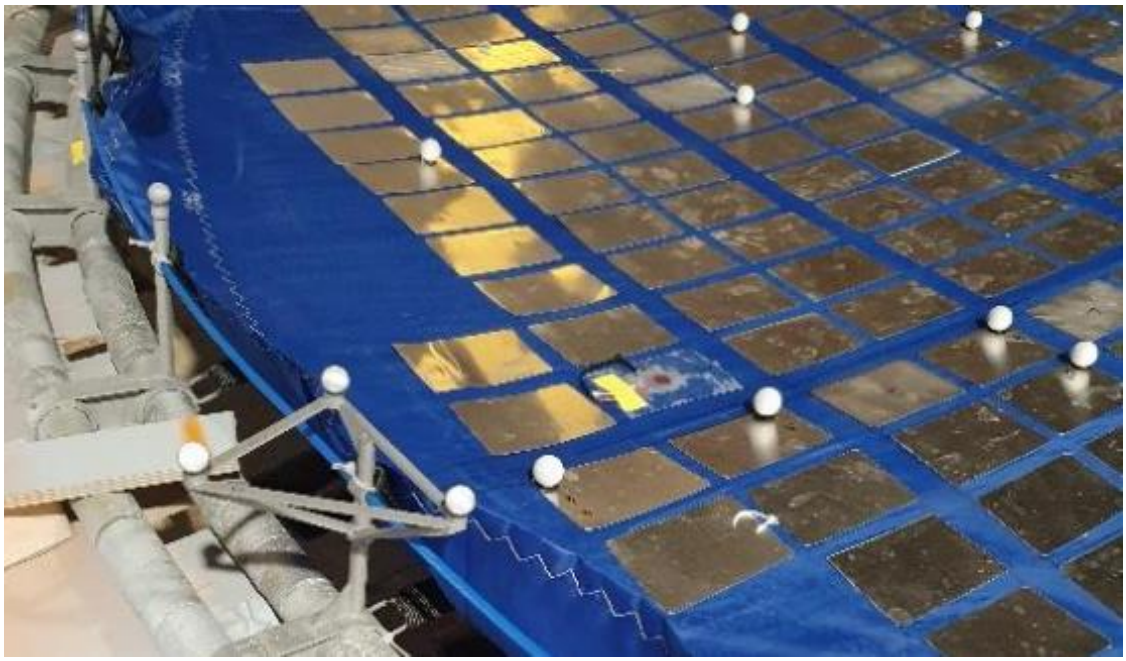

Figure 2 Excerpt of model basin tarpaulin.

An analysis model containing the tarpaulin, collars and bridles and moorings were established as shown in Figure 3.

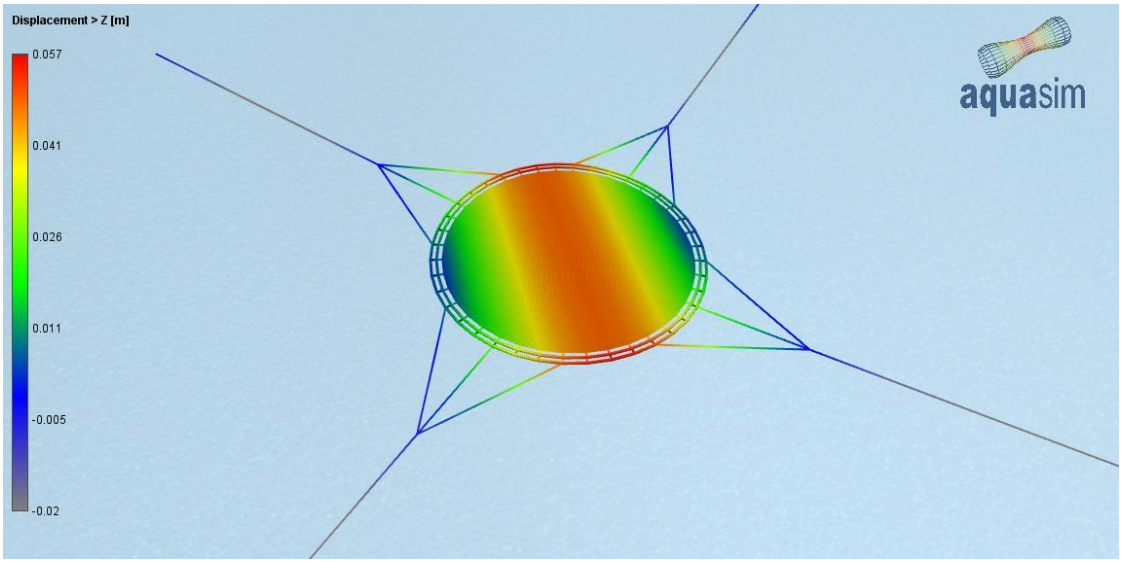

.

Figure 3 FE analysis model of model basin test case. Colors indicates vertical displacement.

This paper presents the theory for analysis of surface tarpaulin included in the FE analysis program AquaSim (Aquastructures 2022). Results from model basin testing compared to the AquaSim analysis are discussed.

2. THEORY

The basic assumption for a surface tarpaulin is that it is laid out along the water line and that it responds to current, and waves as outlined in this paper.

2.1 Static equilibrium

The static equilibrium is calculated by equilibrium between the weight of the tarpaulin and other objects on top of the tarpaulin and hydrostatic pressure from below. For each element there is equilibrium between weights and buoyancy at the water line.

2.2 Loads from current

Define a coordinate system where the z- axis points upwards. Drag forces both due to tangential friction and crossflow can be applied. When the tarp is horizontal, cross flow drag may not be necessary to apply as the surface spring effect is a strong force in the vertical direction. Tangential skin friction drag is represented by:

$$F_{cx} = AC_t \frac{\rho}{2} |u_{tan}| u_x \tag{1}$$

and

$$F_{cy} = AC_t \frac{\rho}{2} |u_{tan}| u_y \tag{2}$$

For drag forces in the *x*- and *y*- direction respectively. A is the area of the element, u_{tan} is the water flow velocity tangential to the element. ρ is the density of water and C_t is the tangential drag coefficient. The water flow velocity includes the relative fluid flow to the tarp caused by both current and waves and the element velocity is subtracted meaning that

$$u = u_w + u_c - u_e \tag{3}$$

Where u_w is the fluid flow velocity caused by waves, u_c by current and u_e is the velocity of the structure. The cross flow drag is calculated as

$$F_N = AC_d \frac{\rho}{2} |u_N| u_N \tag{4}$$

Where C_d is the form drag coefficient, and u_N is the relative flow velocity on the direction normal to the tarp.

2.3 Wave loads

Loads normal to the surface tarpaulin

For a regular wave propagating along the positive x- axis, waves lead to a dynamic time dependent pressure, p_d that for infinite water depth can be expressed by:

$$p_d = \rho g \zeta_a e^{kz} \sin(\omega t - kx) \tag{5}$$

Where ζ_a is the wave elevation, ρ is the density of the fluid, g is the gravitational constant, ω is the wave frequency and k is the wave number $k = \omega^2/g$ for infinite depth and $k\,tanh(kh) = \omega^2/g$ for finite depth. (see e.g Faltinsen 1990 Table 2.3). For finite water depth it can be expressed as:

$$p_d = \rho g \zeta_a \frac{\cosh(z+h)}{\cosh(kh)} \sin(\omega t - kx) \tag{6}$$

The total pressure is the static pressure, plus dynamic pressure and can be formulated as:

$$p = p_d - \rho g z + p_{atm} \tag{7}$$

Forces from water to a submerged body will be the integral of the pressure around the body. We start out with integrating the pressure over the surface, then the Froude Krylov force, F_{FK} can be found as:

$$\vec{F}_{FK} = -\iint_{Sw} p\,\vec{n} ds \tag{8}$$

Where p is the pressure introduced by the undisturbed wave field, $\vec{n}$ is the unit vector normal to the wetted surface S_w. The vertical force is derived from 8:

$$\vec{F}_{FK} = -\iint_{Sw} p\,\vec{z} ds \tag{9}$$

The more the surface tarpaulin follows the wave motions without disturbing it, the less diffraction will be introduced. By choice, diffraction may be added as:

$$\vec{F}_{FK} = -\iint_{Sw} p_D\,\vec{n} ds \tag{10}$$

Where *Sw* is the wetted area and p_D is the pressure introduced by the diffracted wave. The total force to the body is then found as:

$$\vec{F} = \vec{F}_{FK} + \vec{F}_D \tag{11}$$

Loads tangential to the surface tarpaulin

Consider the case where a wave is moving along under a tarp. If the tangential velocity of a tarpaulin at the surface differs from the velocity of the fluid underneath, there will be a boundary layer disturbing the fluid motions similar to seen in Figure 4. Water flow parallel to the tarpaulin will introduce forces. These forces are subdivided to two effects:

1. Tangential drag with a relation between forces and the fluid velocity relative to the tarpaulin, u_t as given in Equation 12.
2. A tangential force caused by tarpaulin sticking to the wave particle motion.

$$F_N = AC_t \frac{\rho}{2} |u_t| u_t \tag{12}$$

The tangential force caused by tarpaulin sticking to the wave particle motion can be viewed as a suction effect where the tarp is sucked to the water at the surface so that it to some degree follows the water particle motion similar to a boundary layer as seen in Figure 4.

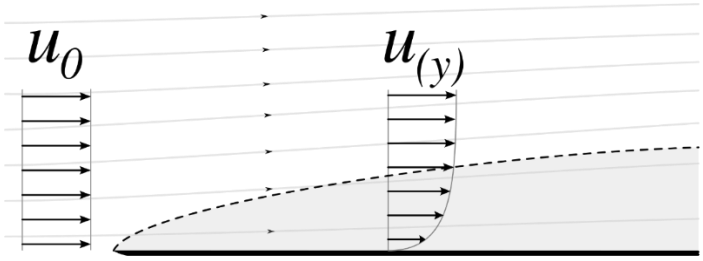

Figure 4 Boundary layer for fluid stream along a plate (from Wiki (2022))

To obtain the tangential forces and response caused by the surface suction effect, a formulation analogous to the flexible tarp fluid load theory outlined in Berstad (2021) is introduced. Consider a tangential flow along a horizontal surface tarp and introduce a surface suction force as:

$$\vec{F}_t = C_s \rho u A \tag{13}$$

where A is the area of the element, ρ is the density of the fluid, u is the horizontal velocity according to linear wave theory (e.g. Faltinsen 1990) Note that for calculation of u, the velocity at $z = 0$ is used at and above $z = 0$, while the velocity decays below the water line according to linear wave theory, i.e

$$u = \omega \zeta_a \frac{cosh(z + h)}{sinh(kh)} sin(\omega t - kx) \tag{13}$$

Below the mean water line at ($z < 0$.). Correspondingly, damping is introduced as:

$$Damp = C_s \frac{\omega}{g} Au \tag{14}$$

With no other forces applied to the tarp in the tangential direction this means the tarp will follow the horizontal fluid particle motion in the wave. This means C_s can be seen as a tarp suction factor for how strongly the tarp sticks to the below water particle parallel to the tarp and C_s is input to the analysis. Note that since it is accounted for that the velocity will be lower below the mean free surface, this introduces an average drift.

As seen from Figure 4, there will be some mass distribution involved when the surface tarp is set in motion and the water sticks to the surface. Intuitively such mass will be proportional to the wavelength. Hence an added mass coefficient proportional to the wavelength is introduced,

$$Am_{hor} = C_{at}\frac{\rho}{\omega^2}\mathrm{A} \tag{15}$$

Where C_{at} is an added mass coefficient representing the mass of the water moving with the tarpaulin. A corresponding force term is:

$$\vec{F}_{Am} = C_{at}\frac{\rho}{\omega^4}Aa \tag{16}$$

Where *a* is the waves acceleration in the horizontal direction. This force term is applied in parallel with the added mass term.

Irregular waves
In irregular velocities and accelerations is calculated from summarizing the components in the spectrum, whereas the peak period of the spectrum is used for damping and added mass terms. The scope of this paper was limited not to compare results for irregular wave testing.

3. MODEL BASIN TESTING COMPARED TO ANALYSIS

3.1 Model basin test setup and analysis model

Figure 5 shows the tarpaulin and floating collars.

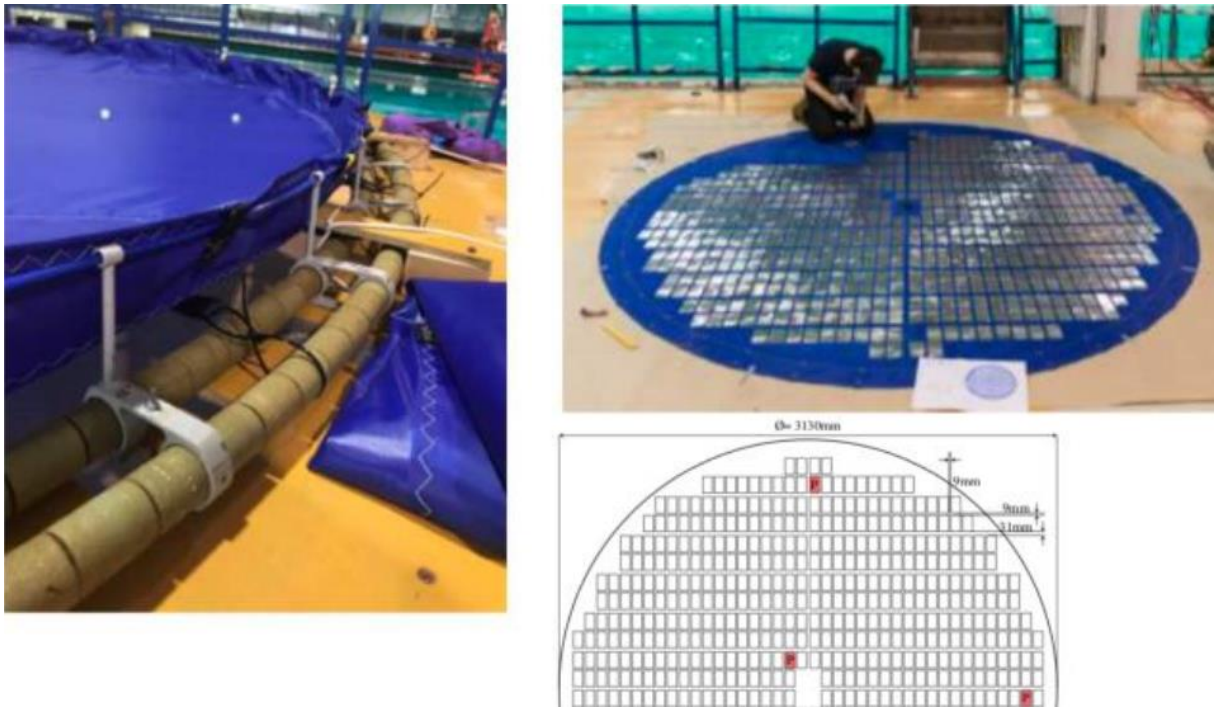

Figure 5 Model test setup. The outer diameter of the tarpaulin is 3130 mm.

Table 1 shows the main particulars of the test arrangement and analysis model.

Table 1 Main particulars for the system

Floater		
# Tubes	2	
Diameter tube	31.3	mm2
Distance between tubes cc	70	mm
Thickness tube	1.84	mm
Elastic module	92	MPa
Density polyethylene	1000	kg/m3
Brackets		
Length (cc)	70	mm
Cross sectional area	76	mm2
Density	958	kg/m3
Elastic module	1000	MPa
2nd area moment of inertia about vertical axis	1305	mm4
Bridles		
Diameter rope	1	mm
Elastic module	210	MPa
Density	954	kg/m3
Load lines		
Diameter rope	1	mm
Elastic module	20	MPa
Density	851	kg/m3

Figure 6 shows the layout of bridles and moorings in the analysis model and Figure 7 shows wave direction (ref Table 3) and tow direction (Table 3 test 11)

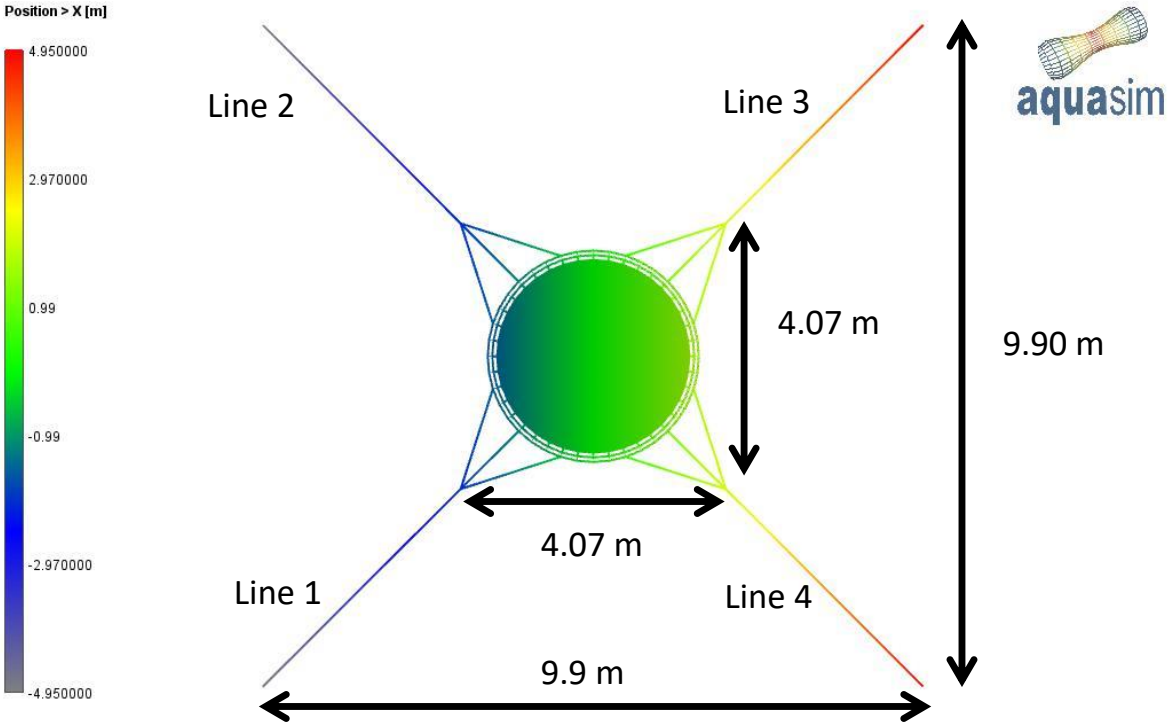

Figure 6 Layout of bridles and mooring lines. Colors represents x- position in analysis model.

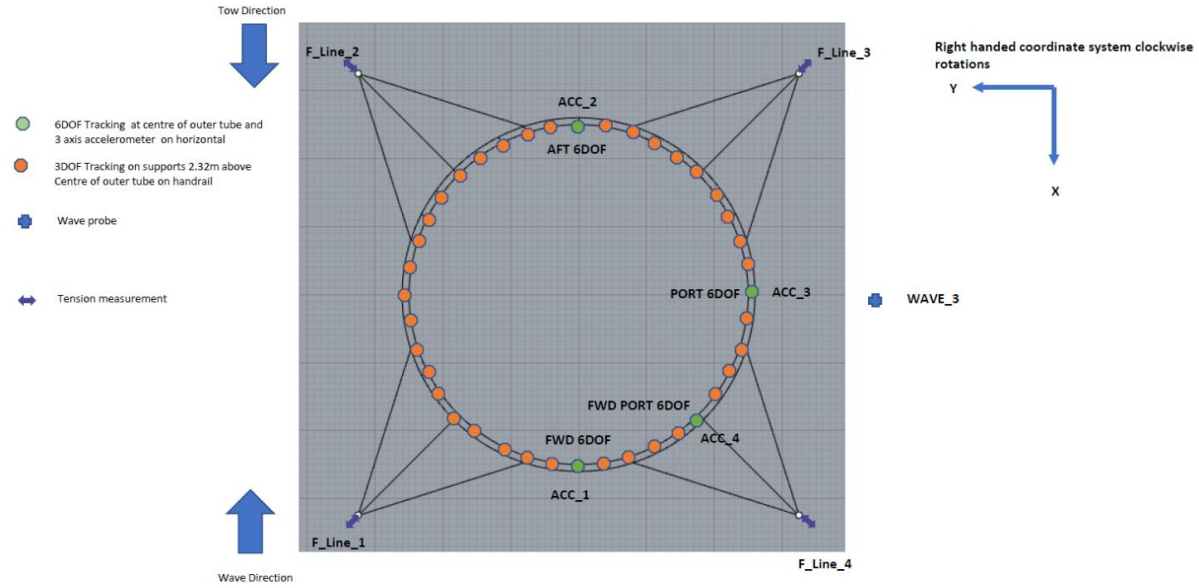

Figure 7 Test arrangement (From Sintef 2021)

The analysis model consists of membrane elements representing the surface tarpaulin, beam elements representing floating collars and clamps and truss elements representing bridles and mooring lines as well as the straps connecting the surface tarpaulin to the floating collars as seen in Figure 8. The surface tarpaulin is discretized to a finite number of 4 noded or 3 noded membrane elements (Aquastructures 2022) as seen in Figure 8 where the colors indicates element number.

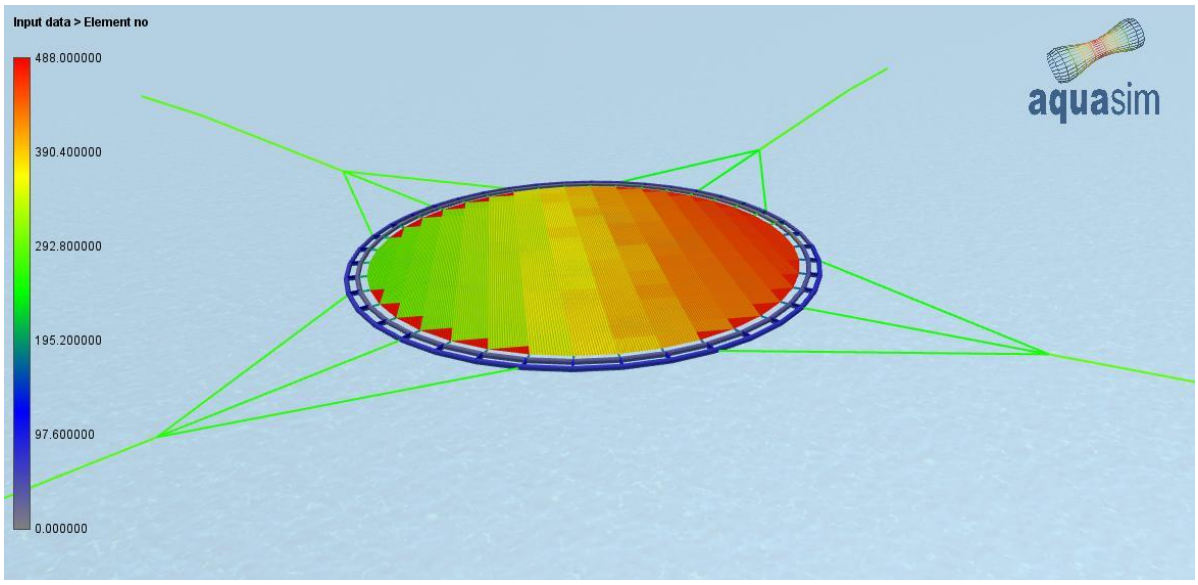

Figure 8 FE element distribution in FE analysis model(Aquastructures 2022)

Table 2 shows hydrodynamic coefficients used in the analysis for the base analysis model. Sensitivity of parameters are investigated. In such case the parameter variations are presented in the corresponding section.

Table 2 Hydrodynamic coefficients

Tarpauline	
Drag coefficient, C_d	0.0085
Surface suction coefficient, C_s	0.0032
Tangential added mass suction coefficient, C_{at}	0.0014
Hydrodynamic damping coefficient (normal)	0.1
Floater	
Drag coefficient outer ring	0.4
Drag coefficient inner ring	0.4
Horizontal damping coefficient	0.0
Bridles	
Drag coefficient	1.2
Added mass coefficient	1
Load lines	
Drag coefficient	1.2
Added mass coefficient	1

3.2 Load cases

Load cases are shown in Table 3

Table 3 Load cases

No	Name	H [m]	T [m]	Uc [m/s]
01	Tension offset			
02	Free decay			
11	Towing			0-0.25
21	Waves	0.0533	2	0
22	Waves	0.055	3.25	0
23	Waves	0.055	4.25	0

3.3 Results load case 01, tension offset

Figure 9 shows force in lines 1 and 4 (F_line_1, F_line_4, see Figure 7).

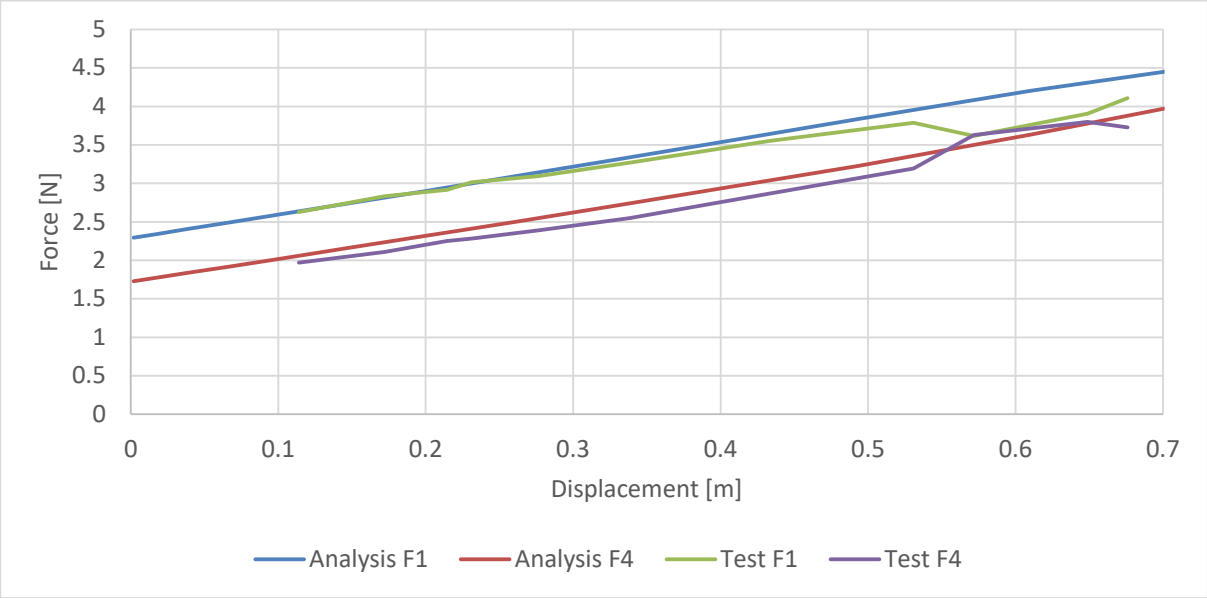

Figure 9 Forces in moorind line 1 and 4. Analysis compared to test results.

As seen from Figure 9 the stiffness of the system corresponds well in analysis vs model basin.

3.4 Results load case 02, Free decay

The free decay test means that the test basin model is pulled sideways before being released and then displacements and forces are logged. In the analysis model this is simulated by introducing a line to a fixed point in the direction the model is pulled as seen in Figure 10.

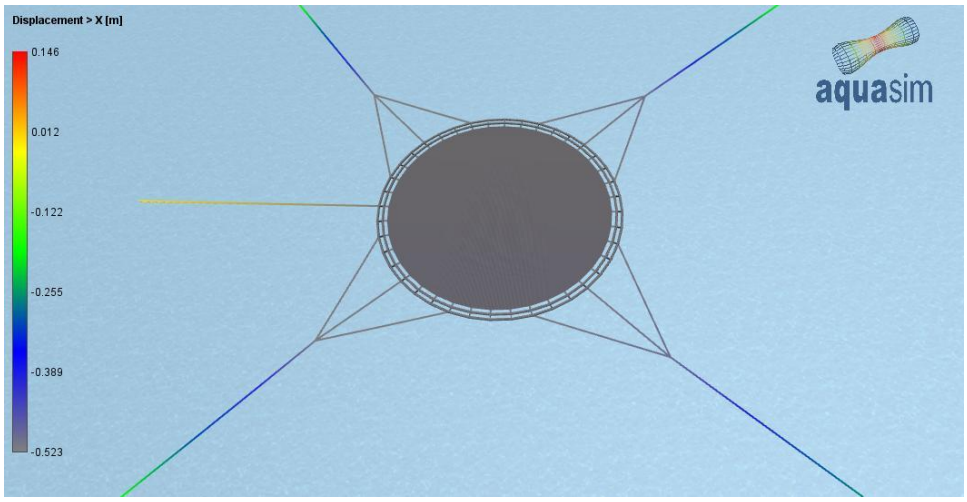

Figure 10 Analysis model for the free decay test

Pretension is applied to this line (pull-line) leading to the tarp moving sideways as in the test. The function "linebreak" is introduced at the pull-line and then decay is seen is Figure 10. The base case with a surface suction coefficient of 0.0032 has been analyzed as well as a case with surface suction coefficient of 0.0017. Results in terms of x- displacement is shown in Figure 11.

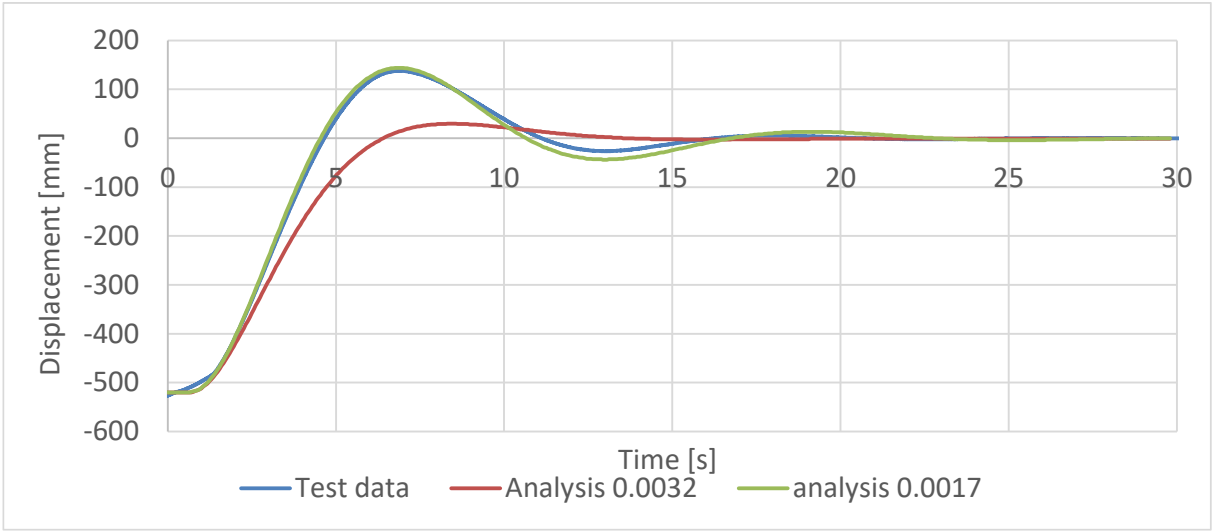

Figure 11 Horizontal displacement decay test.

As seen from Figure 11 the test and analysis correspond well for the case with a suction coefficient of 0.0017. It is typical for model testing that higher damping is seen in wave analysis compared to decay testing and that small changes in damping coefficients with low influence on wave analyses have a large impact in decay testing.

3.5 Results load case 11, towing

In the experimental test campaign, the floater including the horizontal mooring system was towed with various velocities. The numerical model includes a steady current with the same surface velocity as the towing speed. Results are shown in Figure 12. The resulting forces in mooring lines correspond well in general. The force transducer *F4* in the experiment shows a slightly larger increase in tension with increasing towing velocity, but the reason for this is unknown. It could be due to slight variations in mooring line angles, or due to measurement noise. Overall results compare well.

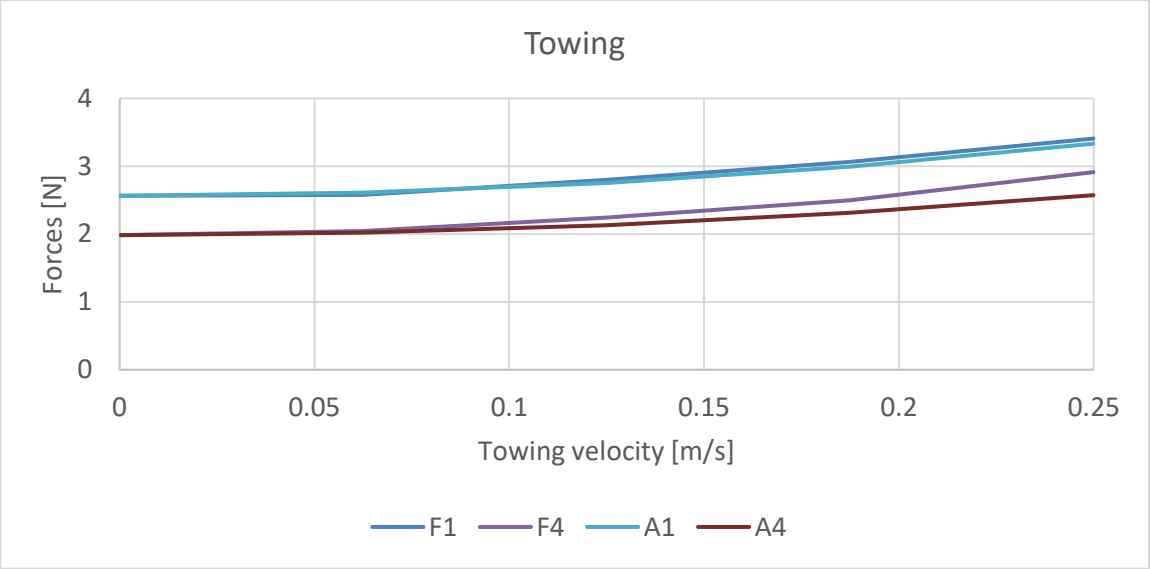

Figure 12 Forces in mooring lines, towing.

3.6 Waves

Results from the analysis with waves are presented such that positive z- value is upwards and positive x- value is in the wave propagation direction. Note that the time series extracts begin when the first waves of the regular wave train encounter the floater. In the experimental tests, the wave heights are gradually ramped up during the first five waves. In the figures an excerpt of the tank test results are shown. In the analysis, the wave height is ramped up during the first two waves, causing the difference in response before reaching steady-state oscillations. Displacement of the floater is measured at the center of the membrane for both experimental and numerical test results.

Case 23

Figure 13 shows comparison of vertical motions and Figure 14 shows comparison of horizontal (surge) motions for case 23. As seen from the figures, results compare well and the variations between the two analysis variations were small.

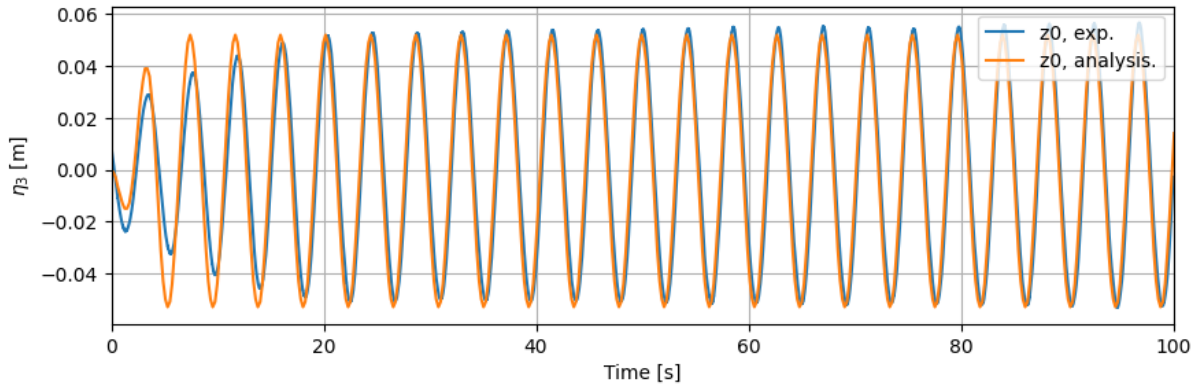

Figure 13 Vertical displacement at tarpaulin centre

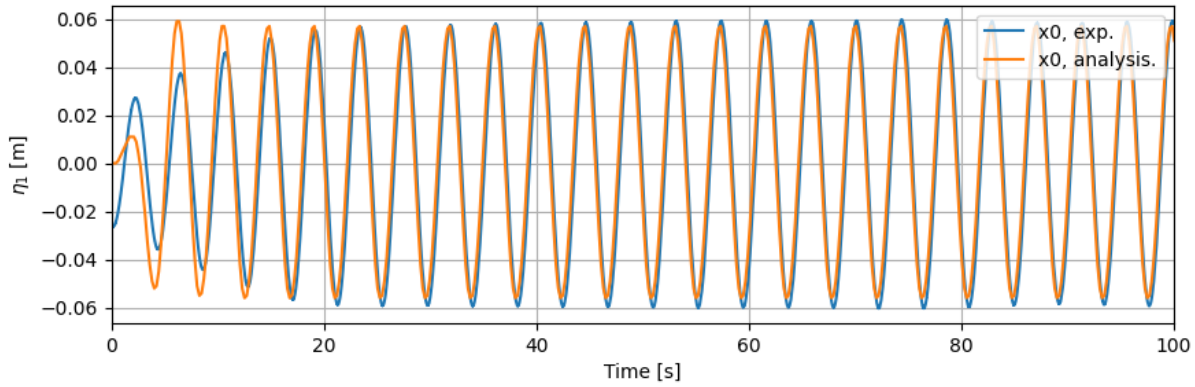

Figure 14 Horizontal displacement at tarpaulin centre

Case 22

Figure 15 shows comparison of vertical motions and Figure 16 shows comparison of horizontal (surge) motions for case 22. As seen from the figures, results compare well also for this case.

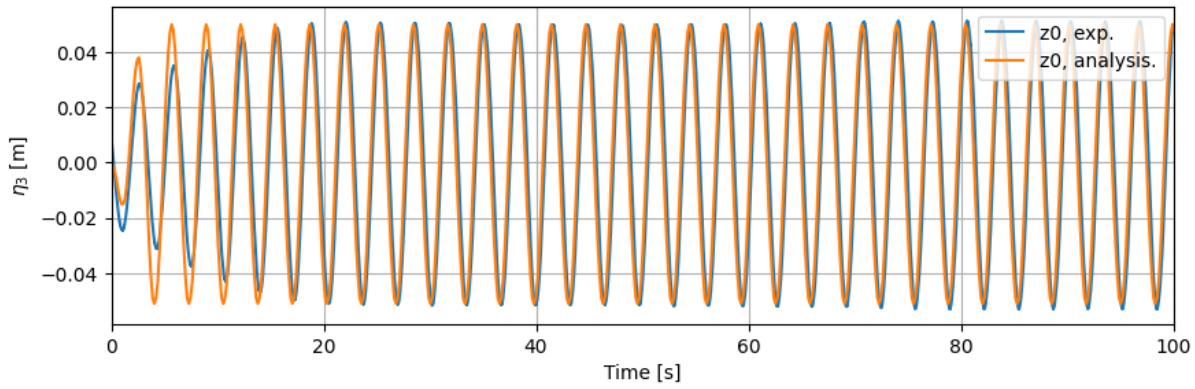

Figure 15 Vertical displacement at tarpaulin centre

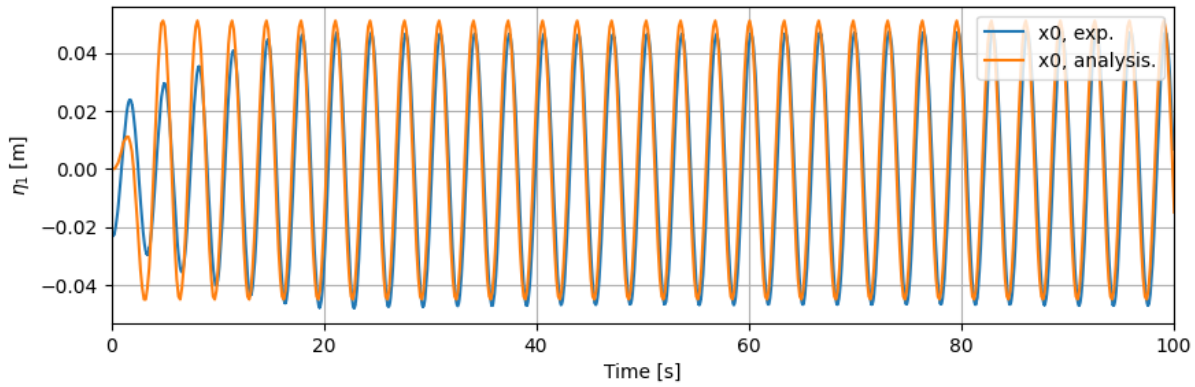

Figure 16 Horisontal motion at tarpaulin centre

Case 21

Figure 17 shows comparison of vertical motions and Figure 18 shows comparison of horizontal (surge) motions for case 21.

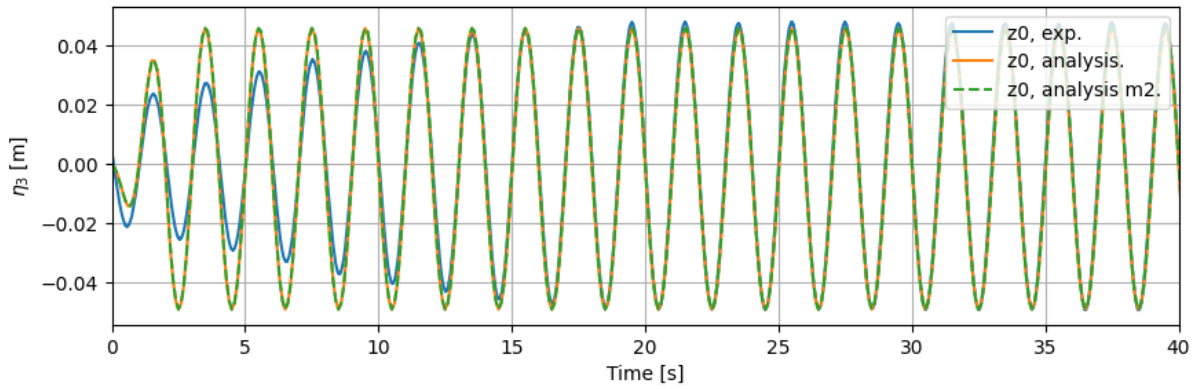

Figure 17 Vertical displacement at tarpaulin centre

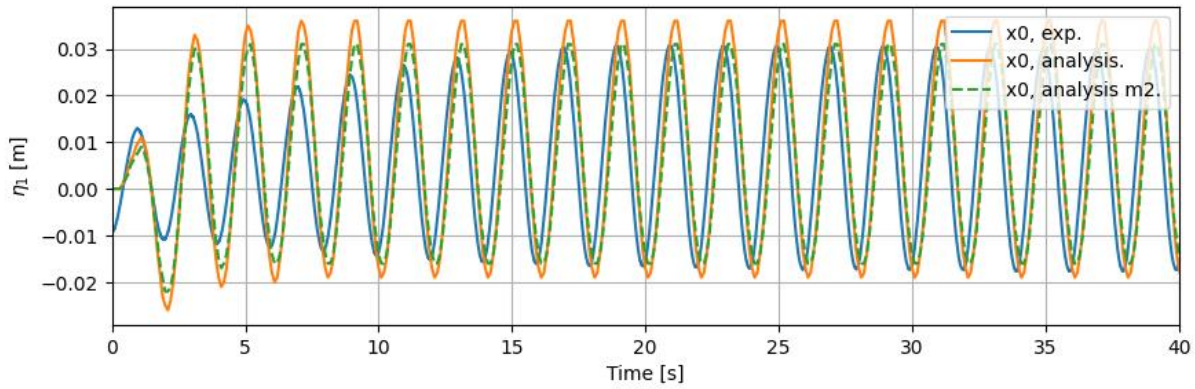

Figure 18 Horizontal displacement at tarpaulin centre

In Figure 17 and Figure 18 the analysis model m2 refers to an analysis model where the suction coefficient was reduced by 33% from 3.2E-3 to 2.13E-3 and the membrane damping coefficient was increased by 33% from 0.1 to 0.133. As seen from the figures, results compare well, but the 2nd variation fitted better with the test data for horizontal motions (Figure 18). This shows the sensitivity of these parameters. It also shows that matching numerical models and experimental models should be carried out for more variations including waves and current combined.

4. CONCLUSIONS

This paper presents analyses compared to model basin testing for a floating solar panel system. The present work shows model basin tank test results compared to FEM simulation using the surface tarpaulin formulation for representation of wave loads presented in this paper. The analysis results compare very well to the model basin results for vertical and horizontal wave induced motion and forces for the investigated floating solar system in regular waves.

Vertical motions are well described by wave pressure regardless of surface suction and skin friction coefficient. For horizontal motions, skin friction as well as surface suction between the tarp and the water is of importance. Surface suction seems to be well accounted for by the surface suction coefficient proposed. It is understood that the surface suction may be strongly influenced by currents. It is hence recommended to carry out further studies to investigate both irregular waves and combination of waves and current.

ACKNOWLEDGEMENTS

This work is supported by the Norwegian Research council, Ocean Sun and Aquastructures. Their support is acknowledged.

REFERENCES

Aquastructures (2022) “AquaSim, AquaEdit user manual” Aquastructures, Kjøpmannsgata 21, N-7013 Trondheim, Norway. https://aquasim.no/files/documentation/User_manual_AquaEdit.pdf

Berstad, Are Johan (2021) “Loads from Waves and Current on flexible tarps” IX International Conference on Computational Methods in Marine Engineering, MARINE 2021. I.M. Viola and F. Brennan (Eds)

Faltinsen, Odd M. (1990) “Sea loads on ships and offshore structures.” Cambridge university press ISBN 0 521 37285 2

Sintef (2021) “Data Summary EU BOOST Towing Tank Tests” PROJECT NO. 302006232 VERSION V1.2 DATE 2021-05-31. Sintef Ocean AS.

Wiki(2022) “ https://en.wikipedia.org/wiki/Boundary_layer”